ResearchGate

See discussions, stats, and author profiles for this publication at: https://www.researchgate.net/publication/279733381

Ultrafast Photoinduced Electron Transfer and Charge Stabilization in Donor–Acceptor Dyads Capable of Harvesting Near-Infrared Light

ARTICLE *in* CHEMISTRY - A EUROPEAN JOURNAL · JUNE 2015

Impact Factor: 5.73 · DOI: 10.1002/chem.201500728 · Source: PubMed

CITATION
1

READS
29

3 AUTHORS, INCLUDING:

Venugopal Bandi
University of North Texas
16 PUBLICATIONS **128** CITATIONS
SEE PROFILE

Habtom Gobeze
University of North Texas
20 PUBLICATIONS **72** CITATIONS
SEE PROFILE

Available from: Venugopal Bandi
Retrieved on: 27 January 2016

ChemPubSoc Europe

DOI: 10.1002/chem.201500728

CHEMISTRY A European Journal Full Paper

Near Infrared Sensitizers

Ultrafast Photoinduced Electron Transfer and Charge Stabilization in Donor–Acceptor Dyads Capable of Harvesting Near-Infrared Light

Venugopal Bandi, Habtom B. Gobeze, and Francis D'Souza*[a]

Abstract: To harvest energy from the near-infrared (near-IR) and infrared (IR) regions of the electromagnetic spectrum, which constitutes nearly 70% of the solar radiation, there is a great demand for near-IR and IR light-absorbing sensitizers that are capable of undergoing ultrafast photoinduced electron transfer when connected to a suitable electron acceptor. Towards achieving this goal, in the present study, we report multistep syntheses of dyads derived from structurally modified BF_2-chelated azadipyrromethene (ADP; to extend absorption and emission into the near-IR region) and fullerene as electron-donor and electron-acceptor entities, respectively. The newly synthesized dyads were fully characterized based on optical absorbance, fluorescence, geometry optimization, and electrochemical studies. The established energy level diagram revealed the possibility of electron transfer either from the singlet excited near-IR sensitizer or singlet excited fullerene. Femtosecond and nanosecond transient absorption studies were performed to gather evidence of excited state electron transfer and to evaluate the kinetics of charge separation and charge recombination processes. These studies revealed the occurrence of ultrafast photoinduced electron transfer leading to charge stabilization in the dyads, and populating the triplet states of ADP, benzanulated-ADP and benzanulated thiophene-ADP in the respective dyads, and triplet state of C_{60} in the case of BF_2-chelated dipyrromethene derived dyad during charge recombination. The present findings reveal that these sensitizers are suitable for harvesting light energy from the near-IR region of the solar spectrum and for building fast-responding optoelectronic devices operating under near-IR radiation input.

Introduction

In the field of solar energy harvesting, photoinduced electron transfer[1] plays a very important role in establishing the usefulness of the newly constructed donor–acceptor systems for building devices for light-into-electricity and light-into-fuel conversion applications[2–5] as well as optoelectronic devices for pertinent applications.[6] In the construction of such donor–acceptor architectures, a biomimetic approach of mimicking natural photosynthesis is often targeted.[2–5] Starting from simple donor–acceptor dyads and moving to more complex multi-modular systems, a number of constructs have been successfully designed and studied in this regard. It has been possible to generate the highly desired long-lived charge-separated states, similar to that found in natural photosynthetic systems,[7] by engineering the energy levels of these systems. However, the majority of such donor–acceptor systems have utilized sensitizers that exhibit absorption and emission in the UV/Vis region of the electromagnetic spectrum, which limits their potential of harvesting energy from the near-IR and IR regions.[1–6,8] Only a handful of near-IR sensitizers, such as π-expanded phthalocyanine derivatives, squaraine compounds, and thieno-pyrrole-fused BODIPY (=4,4-difluoro-4-bora-3a,4a-diaza-*s*-indacenes)[9] have been used successfully. This limitation is due to the tedious multistep synthesis, low reaction yields, reactive intermediates, poor solubility, poor photostability, and limited scope of functionalization of these near-IR sensitizers.

BF_2-chelated dipyrromethene (BODIPY or BDP) and its azadipyrromethene analogue (azaBODIPY or ADP) are fluorophores that are well-known for their synthetic advantages, tunable absorption and emission with high extinction coefficients, and for their ability to modulate redox properties.[10] Accordingly, pristine forms of both BDP and ADP have been employed in building photosynthetic antenna-reaction center model compounds.[11–15] Advantageously, chemical modification of ring periphery with extended π-conjugation or appropriate substituents modulates the HOMO-LUMO levels of these compounds, extending their absorption and emission well into the near-IR portion while retaining their robust physicochemical properties,[16] thus making them ideal candidates to build donor–acceptor systems that are capable of harvesting near-IR light. This has been verified in the present study, first, by synthesiz-

[a] *V. Bandi, H. B. Gobeze, Prof. Dr. F. D'Souza*
Department of Chemistry, University of North Texas
1155 Union Circle, #305070, Denton, TX 76203-5017 (USA)
E-mail: Francis.DSouza@UNT.edu

Supporting information for this article is available on the WWW under http://dx.doi.org/10.1002/chem.201500728. These include all the manuscript figures in color, DPVs of near-IR probes, femtosecond transient absorption spectra of BDP, ADP, BDP-C_{60} and ADP-C_{60} in toluene and benzonitrile, spectra of chemically oxidized BADP and TADP in benzonitrile, fluorescence decay curves of the probes, MS (ESI) of newly synthesized dyads, ^1H and ^{13}C NMR spectra of newly synthesized compounds.

© 2015 Wiley-VCH Verlag GmbH & Co. KGaA, Weinheim

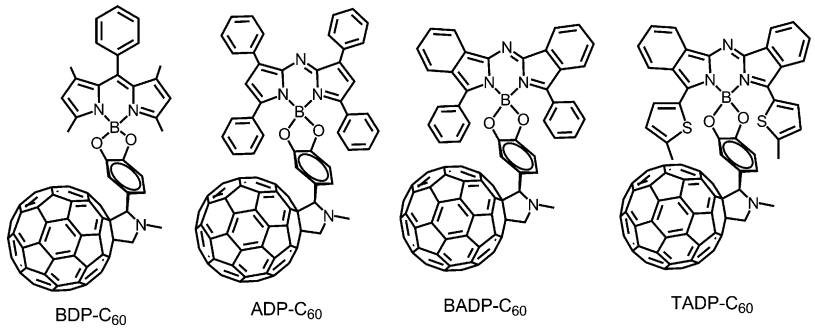

Figure 1. Structures of the BDP-C_{60}, ADP-C_{60}, BADP-C_{60}, and TADP-C_{60} dyads, investigated in the present study.

ing π-extended benzanulated-ADP (BADP) and benzanulated thiophene-ADP (TADP) moieties,[16] and, second, by synthesizing dyads with BDP, ADP, BADP, and TADP moieties covalently linked to the well-known electron-acceptor fullerene (Figure 1).[17]

As shown in Figure 2, both BADP and TADP sensitizers exhibit absorption and emission well into the near-IR region compared with those of traditionally used BDP and ADP sensitizers. That is, BADP revealed absorption and emission maxima at 718 and 751 nm, respectively, while these peaks for TADP are at 774 and 830 nm, respectively. The TADP peaks also revealed substantial broadening, likely due to extended π-conjugation involving peripheral substituents, and absorbance covering a wavelength region of 900 nm. For comparison, BDP absorption and emission peak maxima at 500 and 520 nm and that of ADP at 656 and 691 nm, respectively, in benzonitrile are also shown. The highest Stokes shift of 695 cm^{-1} was observed for BDP, whereas that the lowest was for TADP (240 cm^{-1}), among the series of employed sensitizers. Furthermore, the ability of the newly synthesized BADP-C_{60} and TADP-C_{60} dyads to undergo photoinduced electron transfer leading to charge separated states has been investigated using femtosecond transient absorption spectroscopy.

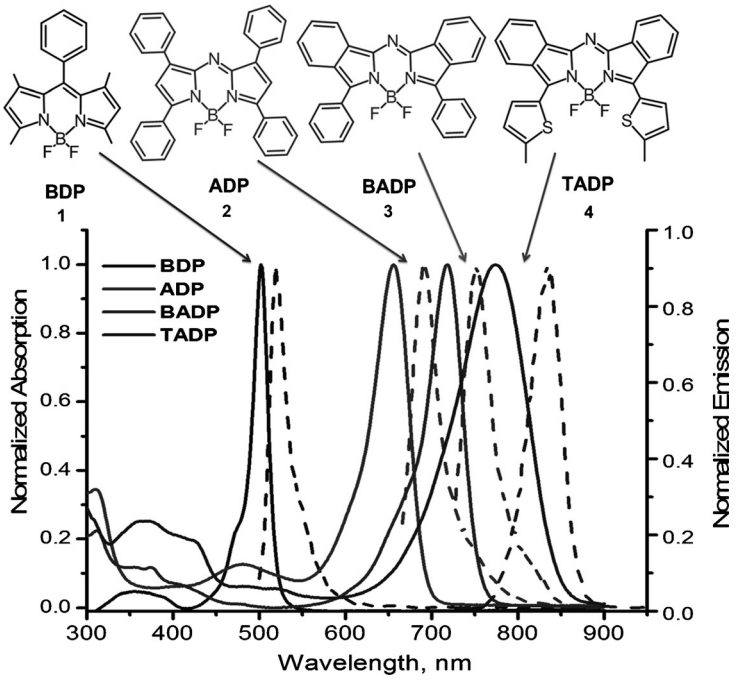

Figure 2. Normalized (to the most intense peak maxima) absorption (solid line) and emission (dashed line) spectra of the investigated sensitizers in benzonitrile. The structure of the corresponding sensitizer is shown at the top.

Results and Discussion

Synthesis of BADP-C_{60} and TADP-C_{60} dyads

The methodology adopted for the synthesis of the dyads is illustrated in Scheme 1; the details are given in the experimental section. Briefly, first, benzo-fused dipyrromethene, having either phenyl or thiophene substituents at the peripheral positions, were synthesized by reacting dicyanobenzene with the corresponding Grignard reagent (phenyl magnesium bromide or 2-methylthiophene magnesium bromide) in diethyl ether at −20 °C followed by heating the reactant mixture to reflux in formamide.[16a] The precipitate formed upon cooling the reaction mixture was treated with boron trifluoride in the presence of diisopropylethylamine in dichloroethane. The BADP and TADP moieties obtained after purification by column chromatography were treated with 3,4-dihydroxybenzaldehyde in the presence of $AlCl_3$ followed by purification of the formyl functionalized BADP and TADP derivatives. Finally, these aldehydes were reacted with fullerene in the presence of sarcosine (N-methyl glycine) in anhydrous toluene according to Prato's method[18] of fulleropyrrolidine synthesis. The purity of the dyads were checked by thin-layer chromatography and the dyads were characterized by ^1H and ^{13}C NMR, ESI-mass, optical spectral and electrochemical methods. The pure products were stored in the dark and fresh solutions were prepared for photochemical measurements.

Optical absorption and fluorescence studies

The absorption spectrum of the dyads in benzonitrile normalized to the most intense peak is shown in Figure 3. Attachment of the fullerene through the central boron (replacing F with O) had a minimum effect on the absorbance behavior, expect for TADP-C_{60}, for which the TADP peak was red-shifted and appeared at 828 nm. A sharp peak at 432 nm, characteristic of fulleropyrrolidine (indicated with an asterisk in Figure 3) was also observed. These results indicate some ground-state interactions between fullerene and modified BODIPY moieties (referred as donor

© 2015 Wiley-VCH Verlag GmbH & Co. KGaA, Weinheim

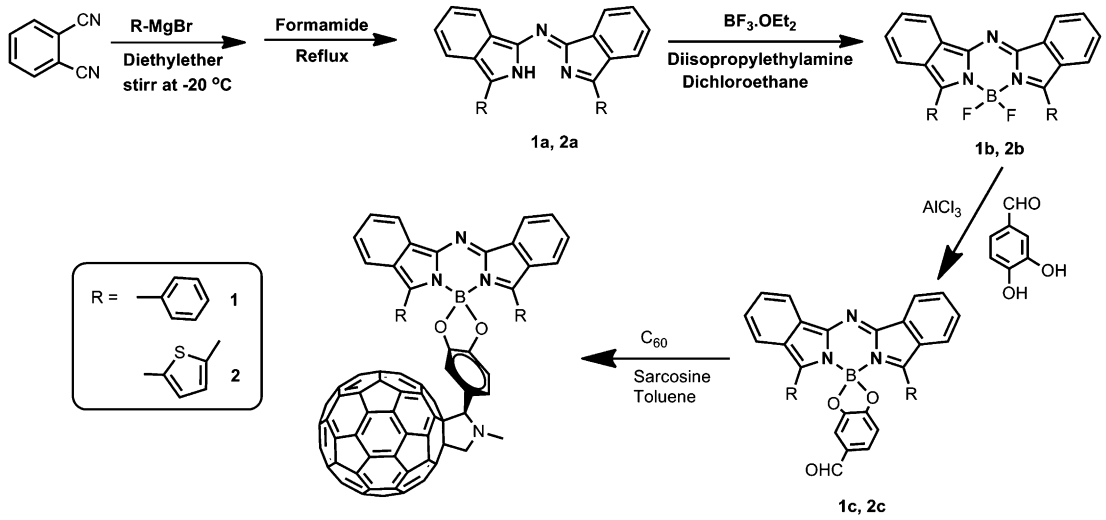

Scheme 1. Synthetic methodology developed for BADP-C_{60} and TADP-C_{60} dyads in the present study.

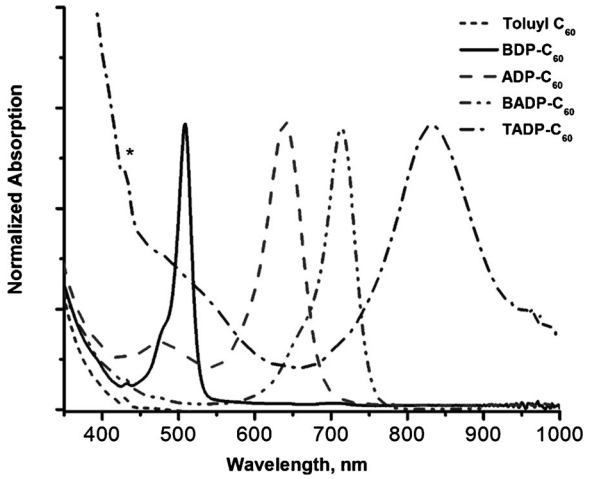

Figure 3. Absorption spectrum of the dyads and fulleropyrrolidine in benzonitrile (normalized to the intense peak maxima).

hereafter) in the dyads. The small spectral shift suggest minimal perturbation of the electronic structure of the donor upon functionalization through the central boron atom. Predictably, fluorescence of the donor moieties (see Figure 2 for the spectra) and 2-tolyl fulleropyrrolidine (in the 720 nm region) in the dyads was found to be fully quenched, indicating the occurrence of excited-state events in the dyads. The absorption spectrum of control compound, 2-phenyl fulleropyrrolidine is also shown in Figure 3. It is important to note that the donor moieties and fulleropyrrolidine both have appreciable absorbance at 400 nm, which is the excitation wavelength of the femtosecond transient spectrometer used in the present study. It may be mentioned here that no spectral evidence for energy transfer from ^{1}BADP* (^{1}TADP*) to fullerene or from $^1C_{60}$* to BADP (or TADP) from steady-state fluorescence measurements was obtained.

Computational and electrochemical studies

Geometry optimization and electronic structure elucidation was performed at the B3LYP/6-31G* level using the Gaussian 03 program[19,20] on the new dyads. The optimized structures along with the first HOMO and LUMO of the new BADP-C_{60} and TADP-C_{60} along with BDP-C_{60} and ADP-C_{60} dyads, for comparison purposes, are shown in Figure 4. The structures were fully optimized on the Born–Oppenheimer potential energy surface. In all the dyads, the donor moiety was found to be almost flat, with a center-to-center distance between the boron atom and the center of fullerene of approximately 10 Å, irrespective of the nature of the modifications. The tetrahedral boron meant that the peripheral substituents on BADP and TADP caused no steric constraints on fulleropyrrolidine. Except for ADP-C_{60}, the LUMO of other three dyads was on fulleropyrrolidine, while for ADP-C_{60}, LUMO + 1 was on fulleropyrrolidine. The HOMO of both BADP-C_{60} and TADP-C_{60} were fully localized on BADP and TADP moieties, while for BDP-C_{60} and ADP-C_{60}, the contributions were also on the bridging catechol segment. This could be a consequence of the moderate level of the MO calculations performed here.[15i] Nevertheless, these studies reveal the formation of BADP$^{\bullet+}$-$C_{60}^{\bullet-}$ and TADP$^{\bullet+}$-$C_{60}^{\bullet-}$ upon excitation of the dyads.

By using differential pulse voltammetry (DPV), the redox properties of the near-IR sensitizers and the dyads were investigated in benzonitrile containing 0.1 M (TBA)ClO_4. The DPV plots of the near-IR sensitizers are shown in Figure S1, and the data are provided in Table 1. For the investigated series of near-IR sensitizers, the oxidation potential followed the trend: BDP ≈ ADP > BADP > TADP, while the reduction potentials followed the trend: BDP > BADP > TADP > ADP. As pointed out earlier,[15c] ADP reduction was easier than reduction of the fulleropyrrolidine, where as that for TADP the reduction overlapped with that of fulleropyrrolidine. The electrochemical HOMO–LUMO gap (potential difference between the first oxidation and first reduction) followed the trend BDP (2.36 V) > ADP (1.56 V) > BADP (1.44 V) > TADP (1.27 V) and were gener-

© 2015 Wiley-VCH Verlag GmbH & Co. KGaA, Weinheim

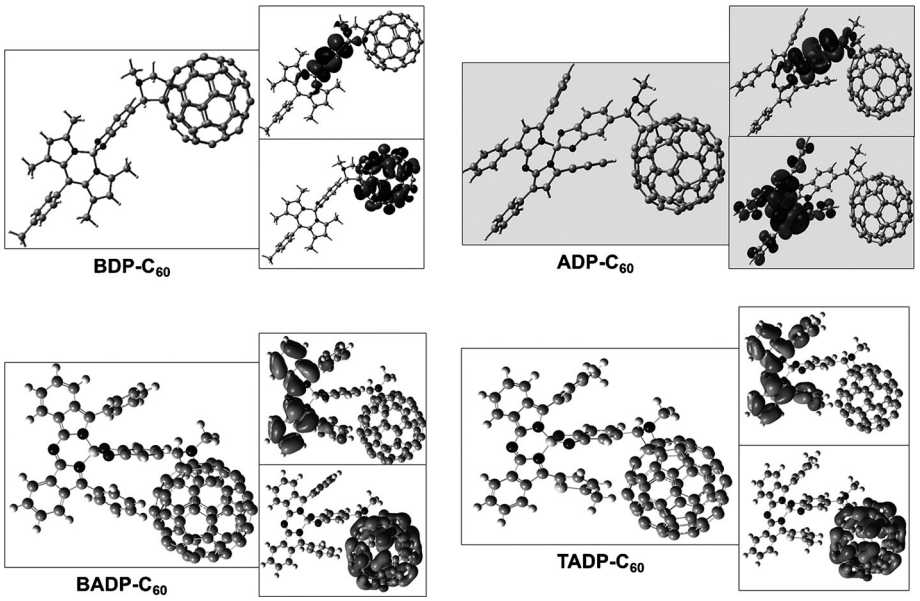

Figure 4. B3LYP/6-31G* optimized structures of the investigated dyads. The HOMO (top) and LUMO (bottom) for each dyad is also shown along with the optimized structure.

Table 1. Redox potentials, free-energy change for charge separation (ΔG_{CS}) and charge recombination (ΔG_{CR}) of the investigated dyads in benzonitrile. Redox potentials of the sensitizers are also given for comparison.

Compd	1st Ox.	1st Red.	2nd Red.	$-\Delta G_{CR}$[a]	$-\Delta G_{CS}$[b,c]	$-\Delta G_{CS}$[b,d]
BDP	0.73	−1.63	–	–	–	–
ADP	0.76	−0.79	−1.54	–	–	–
BADP	0.40	−1.04	−1.75	–	–	–
TADP	0.28	−0.99	−1.74	–	–	–
Toluyl-C_{60}	0.95	−1.02	−1.43	–	–	–
BDP-C_{60}	0.73	−1.02	−1.45	1.69	0.73	0.06
ADP-C_{60}	0.77	−0.78	−1.02	1.73	0.11	0.02
BADP-C_{60}	0.41	−1.01	−1.05	1.36	0.32	0.38
TADP-C_{60}	0.28	−0.99	−1.02	1.21	0.31	0.51

[a] $-\Delta G_{CR} = e(E_{ox} - E_{red}) - \Delta G_S$. [b] $-\Delta G_{CS} = E_{0,0} - (-\Delta G_{CR})$, in which $-\Delta G_S = e^2/4\pi\varepsilon_0\left[\left(1/2R_+ + 1/2R_-\right)\Delta\left(1/\varepsilon_R\right) - \frac{1}{R_{Cc}\varepsilon_R}\right]$, where ΔG_S is the solvation energy, E_{ox} is the first oxidation potential of the dyad, E_{red} is the first reduction potential of the dyad, $E_{0,0}$ is the energy associated with the 0,0 optical transition (midpoint of absorption and emission corresponding to 0,0 transition), being 2.43 eV for BDP, 1.84 eV for ADP, 1.69 eV for BADP, 1.55 eV for TADP, and 1.75 eV for fulleropyrrolidine. R_+ and R_- refer to radii of the cation and anion species, respectively. ε_0 and ε_R refer to vacuum permittivity and dielectric constant of the employed solvent, respectively. R_{Ct-Ct} is the center-to-center distance (distance between boron and center of fullerene) being 10.3 Å for BDP, 10.0 Å for ADP, 9.78 Å for BADP, and 9.66 Å for TADP. The calculated ΔG_S was found to be 0.06 eV for the dyads in benzonitrile. [c] From the singlet excited donor molecule. [d] From the singlet excited fulleropyrrolidine

ally smaller than that calculated from spectral measurements (midpoint of absorption and emission corresponding to the 0,0 transition, see Table 1 footnote for values). This difference was 0.07, 0.28, 0.25, and 0.28 V for BDP, ADP, BADP, and TADP, respectively. These results indicate the probable existence of electronic configurational interactions in the transition, especially for ADP structural analogues.[15j]

The DPVs of the dyads in benzonitrile are shown in Figure 5. To a large extent, the peaks were a superposition of the individual entities, revealing the absence of significant interactions in the ground state between the entities of the dyad. The redox data for the dyads are given in Table 1. By using the redox, computational, and spectral data, free-energy change for charge separation (ΔG_{CS}) and charge recombination (ΔG_{CR}) from the singlet excited donor and fullerene were calculated according to Rehm–Weller's approach (Table 1).[21] The ΔG_{CR} (= E_{RIP}, energy of radical ion-pair) followed the trend: BDP > ADP > BADP > TADP, indicating lower energy storage capability of near-IR sensitizer derived donors. It is also important to note that electron transfer is feasible from both singlet excited sensitizer and singlet excited fulleropyrrolidine to produce donor$^{\bullet+}$-$C_{60}^{\bullet-}$ charge-separated states. Such calculations also reveal that the formation of donor$^{\bullet-}$-$C_{60}^{\bullet+}$ charge-separated states are energetically not possible from either singlet excited donor or fulleropyrrolidine in the present series of dyads.

The energy level diagram showing different photochemical events originating from the singlet excited state of the probes (sensitizer (donor) as well as fulleropyrrolidine) is shown in Figure 6.[22] The energy of charge-separated states generally follow the trend of singlet excited state energy of the donor, except for ADP-C_{60}. Apart from charge separation, singlet-singlet excited energy transfer is also a possibility; however, as pointed out earlier, because of the weak absorbance of fulleropyrrolidine in the emission wavelengths of the near-IR sensitizers, such a process could be considered to be a minor one.[24] In fact, steady-state fluorescence measurements revealed no indication of this event among the series of dyads. The radical ion pairs could relax to the ground state directly; alternatively, they could populate the triplet excited state of the probes (for azaBODIPY derivatives) or fulleropyrrolidine (in the case of BDP-C_{60} dyads) prior to returning to the ground state. To investigate these possibilities, femtosecond and nanosecond transient absorption studies were performed in nonpolar toluene and polar benzonitrile, as discussed below.

Femtosecond transient absorption studies

The transient spectral features of pristine ADP and BDP, shown in Figure S2, have been discussed earlier.[15,25] Briefly, both sensitizers revealed almost instantaneous formation of the singlet-

© 2015 Wiley-VCH Verlag GmbH & Co. KGaA, Weinheim

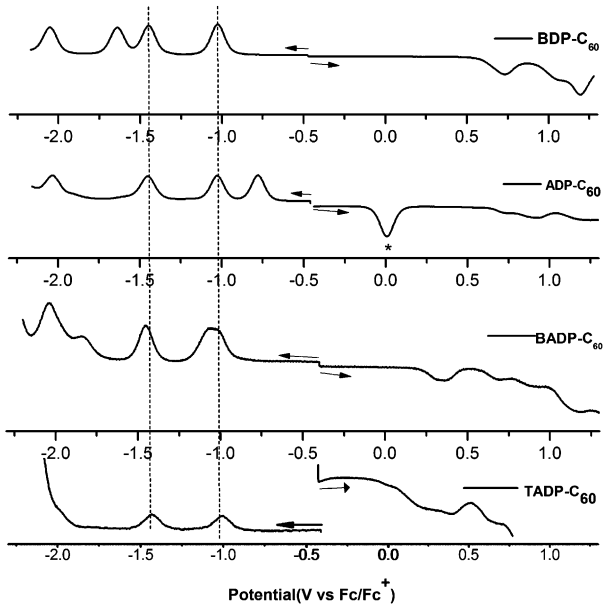

Figure 5. Differential pulse voltammograms of the investigated dyads in benzonitrile, 0.10 M (nBu$_4$N)ClO$_4$. Scan rate = 5 mV s^{-1}, pulse width = 0.25 s, pulse height = 0.025 V. The asterisk in the second panel indicates oxidation process of ferrocene used as an internal standard. The vertical dashed lines show fullerene reductions.

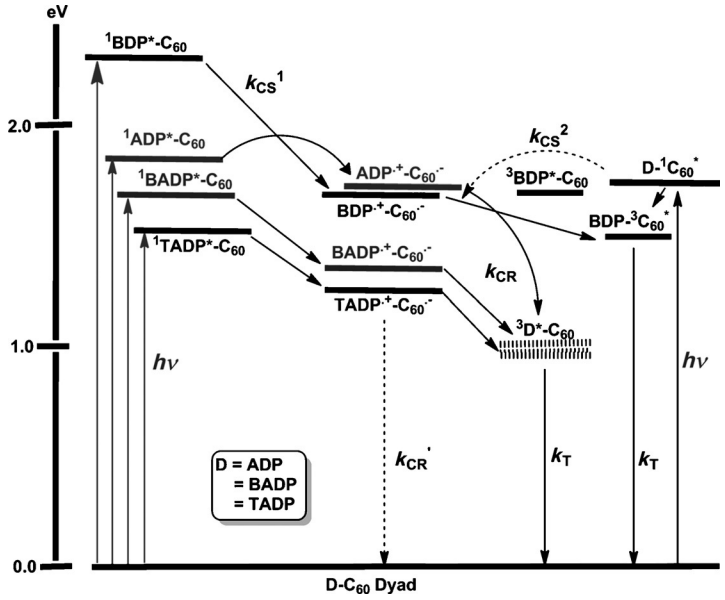

Figure 6. Energy-level diagram showing different photochemical events in the investigated near-IR sensitizer derived donor-fullerene dyads. Solid arrow indicates the most likely process; dashed arrow indicates the less likely process. ^{3}BDP* energy level (E_T = 1.66 eV) was taken from Ref. [24]; for $^3C_{60}$* (E_T = 1.55 eV) the energy level was taken from Ref. [25]. The broken energy level of ^{3}D* refers to an estimated value.

excited state features. In case of BDP, the transient absorption spectra were dominated by pronounced bleaching in the 500 nm range, which was due to depletion of the singlet ground state along with contributions from stimulated emission. The inverse time constant of this peak represents the sum of rate constants for fluorescence, internal conversion, and intersystem crossing. Assuming the latter two processes are minor contributors, the inverse time constant could be attributed to fluorescence. The time constant for the recovery of the 505 nm band in toluene was 2500 ps, while that for the 508 nm band in benzonitrile it was 1896 ps, although the recovery lasted over the 3 ns monitoring time window of our instrument. These values compared with the fluorescence lifetimes of 3.36 and 2.86 ns, respectively, in toluene and benzonitrile for BDP from the time-correlated single-photon counting method (TSCPC; see Figure S5 for decay curves). Similarly, transient absorption spectra of ADP in toluene and benzonitrile revealed the almost instantaneously formed singlet-excited state features with peak maxima at 515 nm and 845 nm range, and minima at 658 nm in toluene, and maxima at 544 and 845 nm range, and minima at 664 nm in benzonitrile, the opposite of the ground-state absorption (including contributions from stimulated emission). Extending the monitoring wavelength window into the near-IR region also revealed a new band in the 1260 nm region, corresponding to the singlet–singlet transition. The time constants for the recovery of the 658 nm peak in toluene was 3204 ps, while that for the 660 nm peak in benzonitrile it was 1825 ps, which are close to their lifetimes of 1.78 and 1.64 ns, respectively, in toluene and benzonitrile determined by using the TCSPC method.

The femtosecond transient spectra of the near-IR probes, BADP and TADP, in toluene and benzonitrile are shown in Figure 7. For BADP, the almost instantly formed singlet ^{1}BADP* revealed positive peaks at 585, 1267(sh), and 1490 nm, and depleted peaks at 716 and 821 nm in toluene (Figure 7a). The origin of the 831 nm peak is not fully apparent at this point. In benzonitrile these peaks were red-shifted by another 5–8 nm. The 716 nm peak corresponded to that of ground-state bleaching and stimulated emission of the probe. Given the similarity to the ADP near-IR band, the 1490 nm peak of BADP has been ascribed to a singlet–singlet transition. This peak decayed with a time constant of 1768 ps in toluene and 1684 ps in benzonitrile, which are close to the lifetimes of 1.91 and 1.89 ns, in toluene and benzonitrile, respectively, determined by using the TCSPC method. The transient spectral features of TADP in toluene and benzonitrile are shown in Figure 6c and d, respectively. Positive peaks at 440, 625 and approximately 1400 nm, and a negative peak at approximately 830 nm were observed, while that in benzonitrile these peaks were located at 455, 620 and approximately 1330 nm, and the negative peak was observed at 842 nm. The near-IR peaks decayed with a time constant of 614 ps in toluene and 608 ps in benzonitrile, which is faster than relaxation of BADP singlet excited state. Singlet excited lifetimes of TADP from the TCSPC method in toluene and benzonitrile were found to be 1.06 and 1.02 ns, respectively (see Figure S5 in the Supporting Information for decay curves).

The femtosecond transient spectra of BDP-C_{60} and ADP-C_{60} in toluene and benzonitrile are shown in Figure S3 in the Sup-

© 2015 Wiley-VCH Verlag GmbH & Co. KGaA, Weinheim

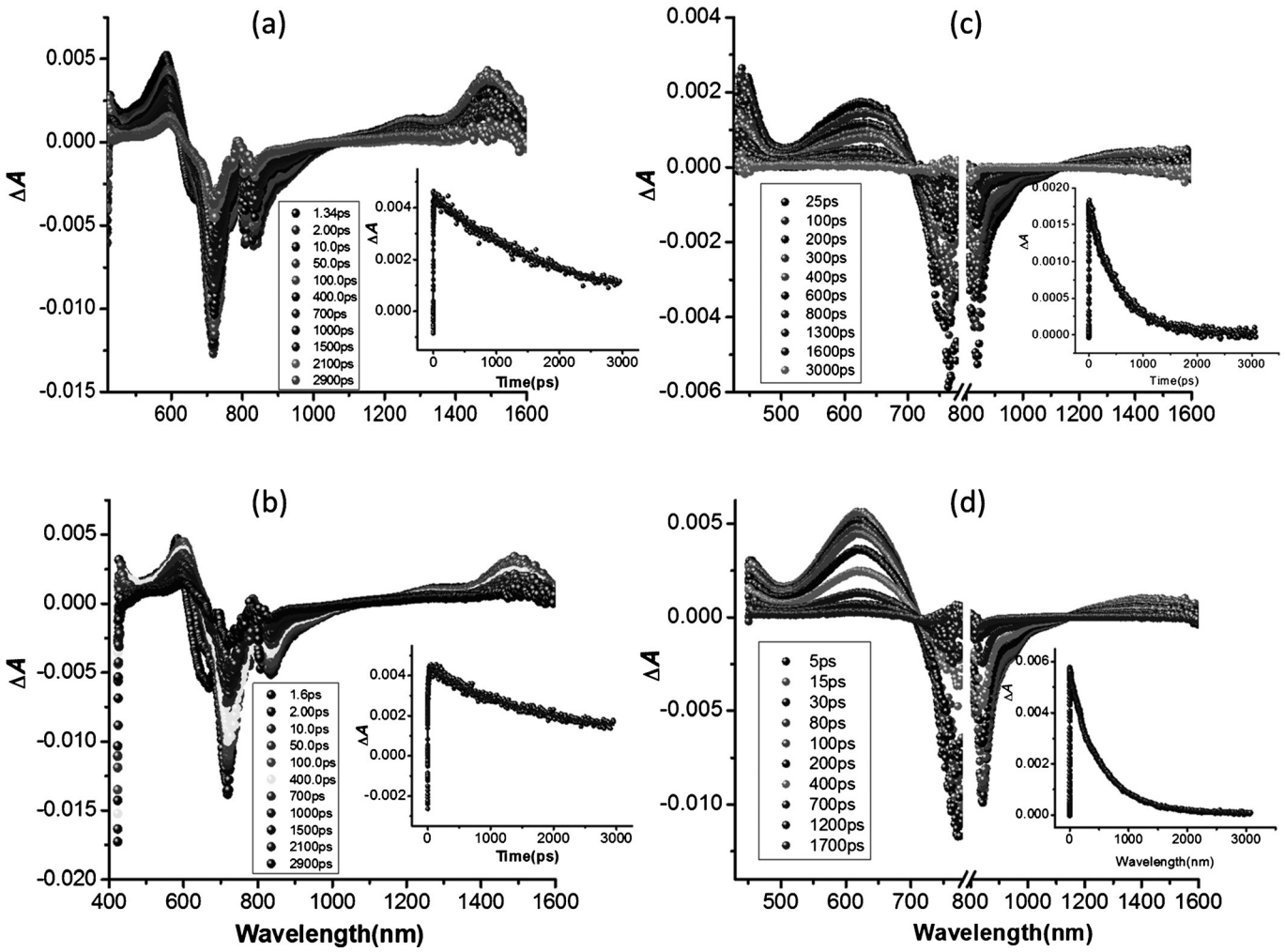

Figure 7. Differential absorption spectra obtained upon femtosecond flash photolysis (400 nm) of BADP in argon saturated (a) toluene (b) benzonitrile, and TADP in (c) toluene and (d) benzonitrile. Figure inset shows the time profile of the 595, 602, 650, and 625 nm peaks of the respective probes.

porting Information. In agreement with our earlier report,[25] charge separation in BDP-C_{60} was evident with the fast decay of the ^{1}BDP* peaks, accompanied by a new peak in the 1020 nm range corresponding to the formation of $C_{60}^{\bullet-}$ (Figure S3a and b). At the excitation wavelength of 400 nm, formation of $^1C_{60}$* was also revealed, as seen by a broad peak in the 900–950 nm region. The formation of $^1C_{60}$* could be due to either direct excitation or ultrafast energy transfer due to closely associated donor–acceptor entities (Dexter type excitation transfer). The rate of charge separation, k_{CS}, and charge recombination, k_{CR}, evaluated by monitoring the rise and decay of the $C_{60}^{\bullet-}$ signal (see Figure S3a and b inset for decay time profiles) are given in Table 2. The decay of the $C_{60}^{\bullet-}$ peak representing charge recombination was accompanied by a new peak at 710 nm, corresponding to the formation of $^3C_{60}$*. These results indicate that the charge-separated state populates the $^3C_{60}$* prior to returning to the ground state. As shown in Figure S3c and d, ADP-C_{60} in toluene and benzonitrile also revealed charge separation,[15c] in which the measured k_{CS} were an order of magnitude higher than that observed for BDP-C_{60} (Table 2). Additionally, the charge recombination involved populating the ^{3}ADP* instead of C_{60}, as revealed by the absence of $^3C_{60}$* in the 700 nm range and an increased absorbance of ^{3}ADP* in the 440 nm range.[15a]

To spectrally identify the oxidation products of BADP-C_{60} and TADP-C_{60} during photochemical charge separation, these

Table 2. Rates of charge separation, k_{CS} and charge recombination, k_{CR} for the investigated dyads in toluene in benzonitrile.

Compd	Solvent	k_{CS} [s^{-1}]	Φ_{CS}[a]	k_{CR} [s^{-1}]	τ_{RIP} [ps]	Ref.
BDP-C_{60}	toluene	7.5×10^{10}	0.993	0.7×10^{9}	1351	this work
	benzonitrile	4.9×10^{10}	0.994	3.2×10^{9}	312	[24]
ADP-C_{60}	toluene	1.0×10^{12}	0.992	3.5×10^{9}	285	this work
	benzonitrile	1.0×10^{12}	0.993	5.0×10^{9}	200	[15c]
BADP-C_{60}	toluene	5.5×10^{10}	0.98	1.2×10^{9}	833	this work
	benzonitrile	21×10^{10}	0.985	11×10^{9}	90	this work
TADP-C_{60}	toluene	0.7×10^{10}	0.42	0.4×10^{9}	2500	this work
	benzonitrile	1.2×10^{10}	0.80	0.7×10^{9}	1428	this work

[a] $\Phi_{CS}=[(1/\tau_f)_{dyad}-(1/\tau_f)_{ref}]/(1/\tau_f)_{dyad}$. See Ref. [26] for details.

© 2015 Wiley-VCH Verlag GmbH & Co. KGaA, Weinheim

dyads were chemically oxidized by using nitrosonium tetrafluoroborate as an oxidizing agent. As shown in Figure S4a, chemical oxidation of BADP in benzonitrile revealed diminished intensity of the BADP peak at 716 nm with no characteristic new bands, perhaps due to low molar extinction coefficient of $BADP^{\bullet+}$. On the contrary, TADP revealed a new peak at 535 nm corresponding to the formation of $TADP^{\bullet+}$.

The femtosecond transient spectra of BADP-C_{60} at the indicated delay times in toluene and benzonitrile are shown in Figure 8. As anticipated from steady-state fluorescence studies, the transient peaks of the singlet excited state deactivated much more rapidly with the appearance of a new transient signature band at 1020 nm due to $C_{60}^{\bullet-}$. A clear peak corresponding to $BADP^{\bullet+}$ was not observed, perhaps due to a low extinction coefficient of that species. The singlet–singlet peak of BADP located at 1490 nm also revealed rapid decay. The k_{CS} and k_{CR} measured by monitoring the growth and decay of the $C_{60}^{\bullet-}$ signal were found to be 5.5×10^{10} and 1.2×10^{9} s^{-1}, respectively. The k_{CS} determined by monitoring the decay of BADP singlet peak at 1490 nm was found to be 4.2×10^{10} s^{-1}, which is close to that obtained from the growth of the $C_{60}^{\bullet-}$ peak. The quantum yields, Φ_{CS}, obtained from k_{CS} values by using the standard procedure[25] were found to be 0.98 in toluene and 0.985 in benzonitrile, respectively. The decay of the radical ion peaks was accompanied by a new peak in the 490–530 nm range, which has been tentatively assigned to the formation of ^{3}BADP* (see above). Interestingly, no peak at 710 nm, corresponding to $^{3}C_{60}$*, was observed, indicating that the charge-separated state does not populate this state prior to returning to the ground state, as envisioned from the energy level diagram in Figure 6.

Femtosecond transient spectra of TADP-C_{60} in the investigated solvents are shown in Figure 9. A negative peak at 830 nm, having contribution from both the ground-state depletion and

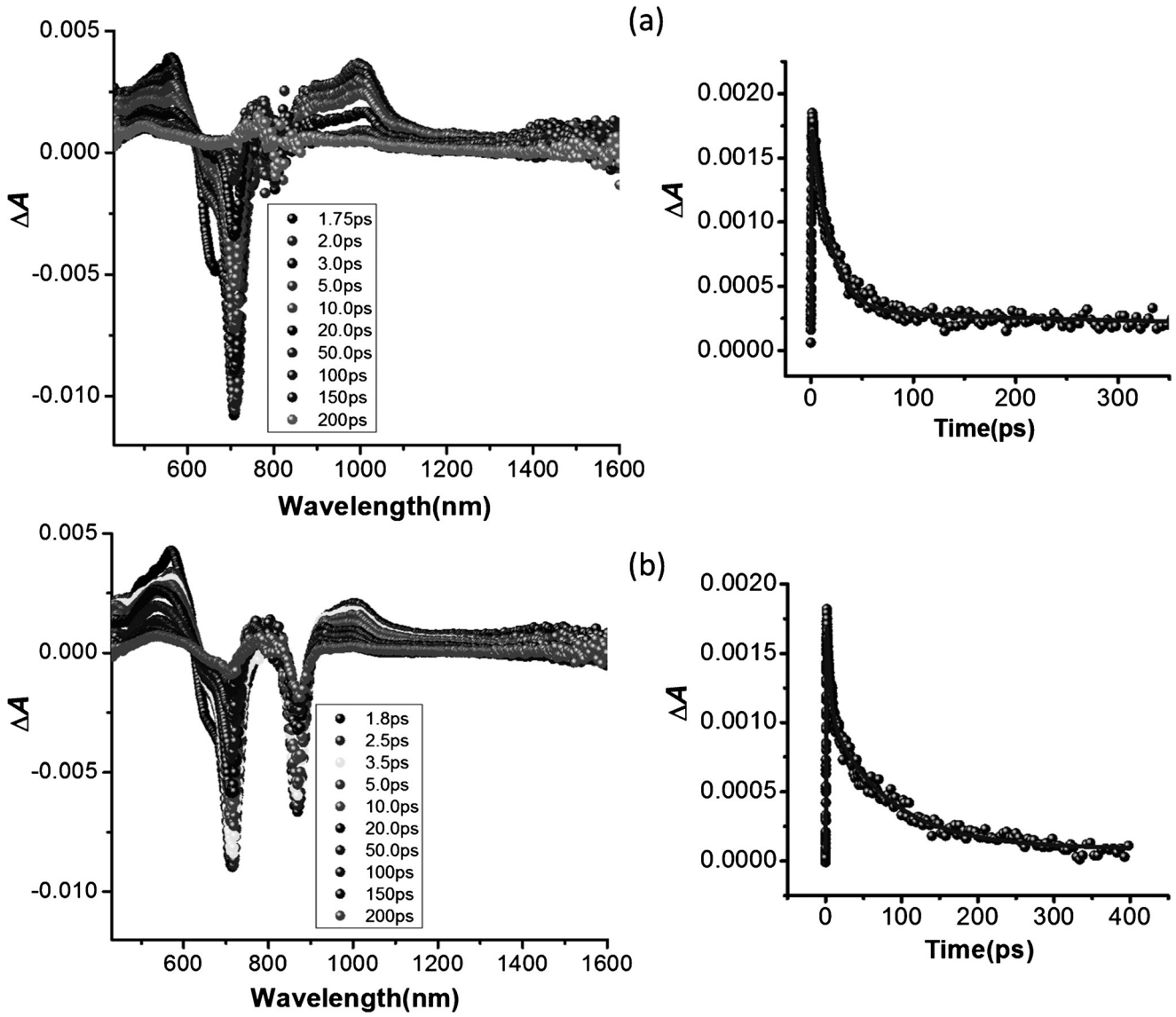

Figure 8. Differential absorption spectra obtained upon femtosecond flash photolysis (400 nm) of BADP-C_{60} in argon saturated (a) toluene and (b) benzonitrile. Figure on the right hand panel shows the time profile of the $C_{60}^{\bullet-}$ peak monitored at 1020 nm.

© 2015 Wiley-VCH Verlag GmbH & Co. KGaA, Weinheim

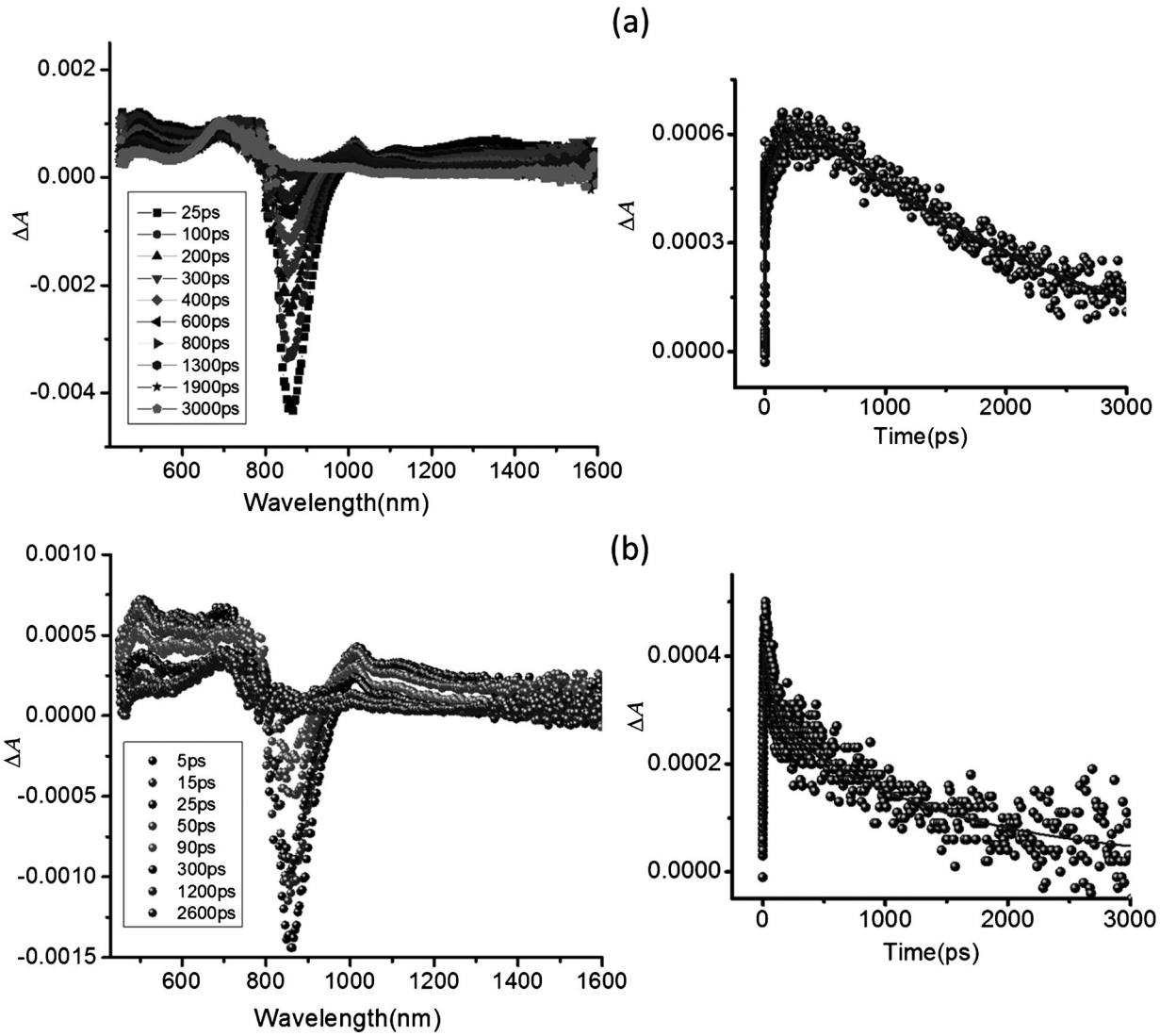

Figure 9. Differential absorption spectra obtained upon femtosecond flash photolysis (400 nm) of TADP-C_{60} in argon saturated (a) toluene and (b) benzonitrile. Figure on the right hand panel shows the time profile of the $C_{60}^{\bullet-}$ peak monitored at 1020 nm.

stimulated emission, was observed. Recovery of this peak is accompanied by new transient bands attributable to the $TADP^{\bullet+}$-$C_{60}^{\bullet-}$ radical ion pair were observed in both solvents. That is, new peaks at 525 nm, corresponding to $TADP^{\bullet+}$ (see Figure S4b for spectra of TDAP during chemical oxidation), and 1020 nm, corresponding to $C_{60}^{\bullet-}$, were observed. As expected, the near-IR band of ^{1}TADP* in the dyad decayed much more rapidly than that in pristine TADP due to an electron-transfer process. The measured kinetic values and quantum yields are provided in Table 2. The decay of the radical ion peak was accompanied by a new peak at 690 nm in toluene and 695 nm in benzonitrile (different from that of $^3C_{60}$* at 710 nm with a shoulder band at 825 nm). These spectral features have been assigned to ^{3}TADP* formation. That is, the $TADP^{\bullet+}$-$C_{60}^{\bullet-}$ radical ion pair populating the ^{3}TADP* prior returning to the ground state, as shown in Figure 6.

Nanosecond transient absorption studies

As mentioned earlier, in the case of BDP-C_{60}[25] and ADP-C_{60},[15c] population of $^3C_{60}$* and ^{3}ADP*, respectively, by the charge-separated species prior to returning to the ground state were observed. The femtosecond transient spectral studies discussed in the previous section revealed populating ^{3}BADP* and ^{3}TADP* by the charge-separation states prior to returning to the ground state. Nanosecond transient absorption spectra were recorded to ascertain this return path of the charge-separated species in the case of these dyads. It may be mentioned here that pristine BADP and TADP revealed very weak, if any, transient bands, leading to lower yields of triplet states, which is a problem that is often encountered with BDP and ADP derivatives. As shown in Figure 10a, nanosecond transient absorption spectra of BADP-C_{60} revealed a peak in the 525 nm range, corresponding to the formation of ^{3}BADP*-C_{60}, whereas in the 700 nm region no spectral signatures corresponding to $^3C_{60}$* was observed. Similar spectral observations were also

© 2015 Wiley-VCH Verlag GmbH & Co. KGaA, Weinheim

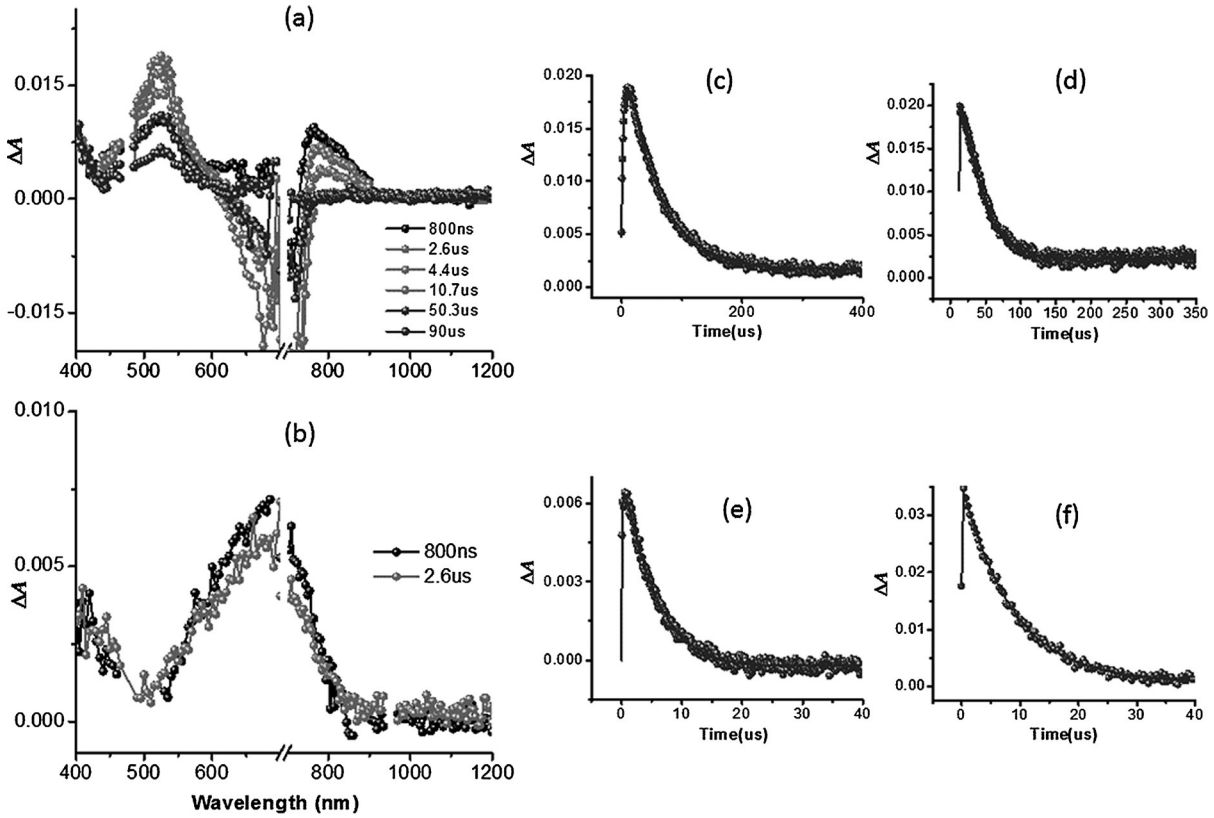

Figure 10. Nanosecond transient absorption spectra ($\lambda_{ex} = 475$ nm of 8 ns pulses) of (a) BADP-C_{60} and (b) TADP-C_{60} in Ar-saturated toluene. Time profile of 525 nm peak of BADP-C_{60} in toluene and benzonitrile are shown in figures (c) and (d), respectively. The time profile of the 680 nm peak of TADP-C_{60} in toluene and benzonitrile are shown in figures (e) and (f), respectively.

made in benzonitrile. From the fitting of the transient band at 525 nm, the decay rate constants of the ^{3}BADP* (k_T) were found to be 1.84×10^4 and 3.05×10^4 s^{-1} in toluene and benzonitrile, respectively. Similarly, the nanosecond transient absorption spectra of TADP-C_{60} revealed a broad peak in the 680 nm range both in toluene and benzonitrile, corresponding to the formation of ^{3}TADP*-C_{60} (Figure 10b). From the fitting of the transient band at 680 nm, the decay rate constants of the ^{3}TADP* (k_T) were found to be 1.13×10^5 and 1.15×10^5 s^{-1} in toluene and benzonitrile, respectively.

An examination of kinetic data for the studied dyads reveal the following: 1) Both k_{CS} and k_{CR} values are higher in polar benzonitrile than those in nonpolar toluene, a trend that generally agrees with the solvation effects on electron transfer rates.[1–2] 2) The k_{CS} values are an order of magnitude higher than k_{CR}, a trend that is often observed for fullerene-based donor–acceptor dyads, implying that k_{CS} falls in the normal region of Marcus parabola, whereas k_{CR} lies in the inverted region.[27] 3) Neither k_{CS} nor k_{CR} follow a trend predicted according to ΔG_{CS} and ΔG_{CR} from Table 1, suggesting other factors, especially reorganization energies, might be different due to different geometries of the modified donor moieties utilized in the present study. 4) The magnitude of charge stabilization, given as τ_{RIP}, suggests better charge stabilization in the TADP-C_{60} dyad. These observations point out that the near-IR sensitizer based donor–acceptor dyads investigated here could be used directly to construct wide-band light energy harvesting devices and also fast-responding optoelectronic devices operating under near-IR light input.

Conclusion

New donor–acceptor dyads utilizing near-IR sensitizers capable of harvesting energy from the near-IR region of the electromagnetic spectrum have been synthesized by using a multistep procedure and characterized by using a variety of physicochemical techniques. The energy level diagram established by using the gathered optical, computational, and electrochemical data revealed the possibility of electron transfer from the singlet excited near-IR sensitizer with possible contributions from the singlet excited fullerene. Accordingly, femtosecond transient absorption studies performed in nonpolar toluene and polar benzonitrile revealed evidence of charge separation in these dyads. The measured rates were found to be very fast for the forward reaction and relatively slow for the reverse reaction, implying charge stabilization. Nanosecond transient spectral studies revealed population of the triplet states of ADP, BADP, and TADP in the respective dyads, and the triplet state of C_{60} in the case of BDP derived dyad. These findings suggest that the near-IR sensitizers developed here are suitable for harvesting light energy from the near-IR region of the solar

© 2015 Wiley-VCH Verlag GmbH & Co. KGaA, Weinheim

spectrum and for relevant technological developments. Further studies along these lines are in progress.

Experimental Section

Chemicals: All the reagents were obtained from Aldrich Chemicals (Milwaukee, WI), and the bulk solvents utilized in the syntheses were obtained from Fischer Chemicals (Plano, TX). Tetra-*n*-butylammonium perchlorate [(nBu$_4$N)ClO$_4$] used in electrochemical studies was obtained from Fluka Chemicals (Ronkonkoma, NY). The syntheses of ADP-C_{60} and BDP-C_{60} were performed according to our earlier procedure.[15c,25]

Synthesis of BADP-C_{60} and TADP-C_{60} dyads: Scheme 1 outlines the general procedure developed for syntheses of these dyads.

Synthesis of 1a and 2a:[16a] In a 250 mL round-bottomed flask, 1,2-dicyanobenzene (5 g, 0.39 mol) and diethyl ether (50 mL) were added. Grignard reagent (1.1 equiv, RMgBr, R = phenyl, 3 M or 2-methylthiophene, 2 M) was added and the mixture was stirred for 30 min at −20 °C under nitrogen. The reaction mixture was stirred for another 3 h at RT. Solvent was evaporated and the reside was heated to reflux with 300 mL formamide (100 mL each for every 30 min) for 3 h. During the reflux, the compound settled as a shiny precipitate. After cooling the reaction mixture, the compound was extracted by filtration and washed with a mixture of methanol/water (2:1). The crude product was used for the next steps without further purification.

Synthesis of BADP 1b:[16a] Compound **1a** (500 mg, 1.258 mmmol) was dissolved in anhydrous dichloroethane (80 mL) and stirred for 15 min under nitrogen. Diisopropylethylamine (0.8 mL, 6.29 mmol) was then added and the mixture was stirred for 1 h followed by addition of boron trifluoride diethyl etherate (0.7 mL, 6.29 mmol). The mixture was heated to reflux under N_2 for 4 h, then cooled to RT, diluted with CH_2Cl_2, and washed with water. The organic layer was separated, dried over Na_2SO_4, and evaporated to dryness. The residue was purified by column chromatography on silica gel (CH_2Cl_2/hexane, 1:1) to give **1b** as a dark-green solid. Yield: 250 mg (45%); ^{1}H NMR (400 MHz, $CDCl_3$): $\delta = 8.10$ (d, $J = 13.6$ Hz, 2H; Ar-H), 7.90 (d, $J = 12$ Hz, 2H; Ar-H), 7.77 (m, 4H; Ar-H), 7.50 (m, 8H; Ar-H), 7.30 ppm (d, 2H; Ar-H); MS (ESI, −, MeOH): *m/z* calcd for $C_{28}H_{18}BF_2N_3$: 446.15; found: 445.15.

Synthesis of BADP-aldehyde 1c: Compound **1b** (136 mg, 0.304 mmol) was dissolved in anhydrous CH_2Cl_2 (30 mL) and stirred under nitrogen for 15 min. $AlCl_3$ (203 mg, 1.522 mmol) was then added and the solution was stirred for 30 min before the addition of 3,4-dihydroxybenzaldehyde (210 mg, 1.520 mmol). The mixture was stirred for 30 min and the reaction mixture was flushed through deactivated basic alumina column with CH_2Cl_2 as eluent. The crude product was further purified by column chromatography (silica; CH_2Cl_2/hexanes, 1:1) to give **1c**. Yield: 80 mg (48%); ^{1}H NMR (400 MHz, $CDCl_3$): $\delta = 9.56$ (s, 1H; aldehyde-H), 8.10 (d, $J = 11.2$ Hz, 2H; Ar-H), 7.60–7.56 (m, 4H; Ar-H), 7.52–7.48 (m, 8H; Ar-H), 7.32 (d, $J = 8$ Hz, 2H; Ar-H), 7.0–6.9 ppm (m, 5H; Ar-H, dioxyaryl-H).

Synthesis of BADP-C_{60} 1: To a solution of C_{60} (103 mg, 0.143 mmol) in anhydrous toluene (100 mL), sarcosine (22 mg, 0.246 mmol) and **1c** (26 mg, 0.047 mmol) were added. The solution was heated to reflux for 24 h and the solvent was removed under vacuum. The residue was purified by column chromatography (silica; ethyl acetate/CH_2Cl_2, 1:4) to give **1**. Yield: 15 mg (24%); ^{1}H NMR (400 MHz, $CDCl_3$ and CS_2): $\delta = 8.12$–8.06 (m, 5H; Ar-H), 7.52–7.46 (m, 7H; Ar-H), 7.34–7.28 (m, 9H; Ar-H, dioxyaryl-H), 4.75 (d, $J = 4$ Hz, 1H; fulleropyrrolidine-H), 4.55 (s, 1H; fulleropyrrolidine-H), 4.05 (d, 1H; fulleropyrrolidine-H), 2.55 ppm (s, 3H; fulleropyrrolidine-H); ^{13}C NMR (500 MHz, $CDCl_3$ and CS_2): $\delta = 174$, 148, 146–144(m), 144–142(m), 140,140–198(m), 136, 131, 129, 128, 127, 124, 122, 70, 69, 57, 34, 32, 31, 30–29 (m), 28–27 (m), 27–26 (m), 25, 23, 19, 14 ppm; MS (ESI, +, MeOH): *m/z* calcd for $C_{95}H_{29}BN_4O_2$: 1331.20; found: 804.5 [$C_{65}H_{10}N$, fulleropyrrolidine fragment], 454.3 [$C_{29}H_{21}BN_3O_2$, BADP fragment].

Synthesis of TADP 2b: Compound **2a** (500 mg) was dissolved in anhydrous dichloroethane (80 mL) and stirred for 15 min under nitrogen. Diisopropylethylamine (1 mL, 6.05 mmol) was added and the mixture was stirred for 1 h followed by addition of boron trifluoride diethyl etherate (1 mL, 8.1 mmol). The mixture was heated to reflux under N_2 for 4 h, then the mixture was cooled to RT, diluted with CH_2Cl_2, and washed with water. The organic layer was separated, dried over Na_2SO_4, and evaporated to dryness. The residue was purified by column chromatography on silica gel (CH_2Cl_2/hexane, 1:1) to give **2b** as a dark-green solid. Yield: 150 mg (27%); ^{1}H NMR (400 MHz, $CDCl_3$): $\delta = 8.18$–8.00 (m, 6H; Ar-H), 7.54–7.50 (t, $J = 16$ Hz, 2H; Ar-H), 7.36–7.30 (t, $J = 24$ Hz, 2H; thiophene-H), 6.94 (d, $J = 5.9$ Hz, 2H; thiophene-H), 2.58 ppm (s, 6H; methyl-H).

Synthesis of TADP-aldehyde 2c: Compound **2b** (100 mg, 0.205 mmol) was dissolved in anhydrous CH_2Cl_2 (30 mL) and the solution was stirred under nitrogen for 15 min. $AlCl_3$ (137 mg, 1.027 mmol) was added and the solution was stirred for 30 min before the addition of 3,4-dihydroxybenzaldehyde (142 mg, 1.028 mmol). The mixture was stirred for 30 min then flushed through deactivated basic alumina as a filter column (CH_2Cl_2 as eluent). The crude product was further purified by column chromatography (silica; CH_2Cl_2) to give the product **2c**. Yield: 50 mg (42%); ^{1}H NMR (400 MHz, $CDCl_3$): $\delta = 9.50$ (s, 1H; aldehyde-H), 8.30–8.14 (m, 6H; Ar-H), 7.56 (m, 2H; Ar-H), 7.35 (t, $J = 3.5$ Hz, 2H; Ar-H), 7.10 (d, $J = 11.8$ Hz, 2H; dioxyaryl-H), 6.95 (d, $J = 1.4$ Hz, 2H; thiophene-H), 6.80 (d, $J = 3.8$ Hz, 1H; dioxyaryl-H), 2.68 ppm (s, 6H; methyl-H).

Synthesis of TADP-C_{60} 2: To a solution of C_{60} (60 mg, 0.674 mmol) in anhydrous toluene (120 mL), sarcosine (60 mg, 0.674 mmol) and **2c** (75 mg, 0.128 mmol) were added. The solution was heated to reflux for 24 h and the solvent was removed under vacuum. The residue was purified by column chromatography (silica; CH_2Cl_2/toluene 1:3) to give **2**. Yield: 30 mg (18%); ^{1}H NMR (400 MHz, $CDCl_3$): $\delta = 8.28$ (d, $J = 12$ Hz, 2H; Ar-H), 7.88 (d, $J = 12$ Hz, 2H; Ar-H), 7.72–7.64 (m, 4H; Ar-H), 7.54–7.48 (m, 5H; thiophene-H, dioxyaryl-H), 7.10 (d, $J = 19$ Hz, 2H; thiophene-H), 4.55 (s, 1H; fulleropyrrolidine-H), 4.42 (d, $J = 4$ Hz, 1H; fulleropyrrolidine-H), 3.80 (s, 1H; fulleropyrrolidine-H), 2.80 (s, 3H; fulleropyrrolidine-H), 2.56 ppm (s, 6H; methyl-H); MS (ESI, +, MeOH): *m/z* calcd for $C_{95}H_{27}BN_4O_2S_2$: 1331.20; found: 1151.8 [M-thiophene units], 467.1 [TADP].

Spectral measurements: The UV/Vis and near-IR spectral measurements were carried out with a Shimadzu 2550 UV/Vis spectrophotometer or a Jasco V-670 spectrophotometer. The steady-state fluorescence emission was monitored with a Varian (Cary Eclipse) fluorescence spectrophotometer or a Horiba Jobin Yvon Nanolog spectrofluorimeter equipped with PMT (for UV/Vis) and InGaAs (for near-IR) detectors. The fluorescence lifetimes were measured with the Time Correlated Single Photon Counting (TCSPC) option with nano-LED excitation sources on the Nanolog. A right angle detection method was used for both steady-state and time-resolved emission measurements at RT. All the solutions were purged prior to spectral measurements by using nitrogen gas. ^{1}H NMR studies were carried out with a Bruker 400 MHz spectrometer. Tetramethylsilane (TMS) was used as internal standard.

The computational calculations were performed by B3LYP methods with the GAUSSIAN 03 software package.[19] The HOMO and LUMO orbitals were generated with the GaussView program.

© 2015 Wiley-VCH Verlag GmbH & Co. KGaA, Weinheim

Electrochemistry: Differential pulse voltammetry was recorded with a Princeton Applied Research potentiostat/galvanostat Model 263A using a three-electrode system. A platinum button electrode was used as the working electrode, a platinum wire served as the counter electrode, and an Ag/AgCl electrode was used as the reference electrode. Ferrocene/ferrocenium redox couple was used as an internal standard. All the solutions were purged prior to electrochemical and spectral measurements with nitrogen gas.

Femtosecond laser flash photolysis: Femtosecond transient absorption spectroscopy experiments were performed with an Ultrafast Femtosecond Laser Source (Libra) by Coherent incorporating diode-pumped, mode locked Ti:Sapphire laser (Vitesse) and diode-pumped intra cavity doubled Nd:YLF laser (Evolution) to generate a compressed laser output of 1.45 W. For optical detection, a Helios transient absorption spectrometer coupled with femtosecond harmonics generator, both provided by Ultrafast Systems LLC, was used. The source for the pump and probe pulses were derived from the fundamental output of Libra (compressed output 1.45 W, pulse width 100 fs) at a repetition rate of 1 kHz. 95% of the fundamental output of the laser was introduced into harmonic generator, which produces second and third harmonics of 400 and 267 nm besides the fundamental 800 nm for excitation, while the rest of the output was used for generation of white light continuum. In the present study, the second harmonic 400 nm excitation pump was used in all the experiments. Kinetic traces at appropriate wavelengths were assembled from the time-resolved spectral data. Data analysis was performed with Surface Xplorer software supplied by Ultrafast Systems. All measurements were conducted in degassed solutions at 298 K.

Nanosecond laser flash photolysis: The studied compounds were excited with a Opolette HE 355 LD pumped by a high energy Nd:YAG laser with second and third harmonics OPO (tuning range 410–2200 nm, pulse repetition rate 20 Hz, pulse length 7 ns) with the powers of 1.0 to 3 mJ per pulse. The transient absorption measurements were performed with a Proteus UV/Vis-NIR flash photolysis spectrometer (Ultrafast Systems, Sarasota, FL) with a fiberoptic delivered white probe light and either a fast rise Si photodiode detector covering the 200–1000 nm range or a InGaAs photodiode detector covering 900–1600 nm range. The output from the photodiodes and a photomultiplier tube was recorded with a digitizing Tektronix oscilloscope. Data analysis was performed with Surface Xplorer software supplied by Ultrafast Systems.

Acknowledgements

This work was supported by the National Science Foundation (Grant No. 1401188 to F.D.).

Keywords: donor–acceptor systems · electron transfer · energy conversion · fullerenes · sensitizers

[1] a) H. Taube, *Electron Transfer Reactions of Complex Ions in Solution*, Academic Press, New York, **1970**; b) J. R. Bolton, N. Mataga, G. McLendon, *Advances in Chemical Series* **1991**, *228*, 1; c) *Electron Transfer in Chemistry and Biology: An Introduction to the Theory* (Eds.: A. M. Kuznetsov, J. Ulstrup), Wiley, New York, **1998**; d) *Photoinduced Electron Transfer, Vols. A–D* (Eds.: M. A. Fox, M. Chanon), Elsevier, Amsterdam, **1988**; e) *Topics in Current Chemistry: Photoinduced Electron Transfer, Vol. 156–157* (Ed.: J. Mattay), Springer, Berlin, **1990**; f) *Electron Transfer: from Isolated Molecules to Biomolecules* (Eds.: J. Jortner, M. Bixson), parts 1 and 2, John Wiley, New York, **1999**, p. 107; g) *Electron Transfer in Chemistry, Vols. 1–4* (Ed.: V. Balzani), Wiley-VCH, Weinheim, **2001**–**2002**.

[2] a) M. R. Wasielewski, *Chem. Rev.* **1992**, *92*, 435; b) G. J. Meyer, *Prog. Inorg. Chem.* **1997**, *44*, 167; c) P. Qu, G. J. Meyer in *Electron Transfer in Chemistry, Vol. 4* (Ed.: V. Balzani), **2001**, p. 353; d) W. Leibl, P. Mathis, *Electron Transfer in Photosynthesis. Series on Photoconversion of Solar Energy* **2004**, *2*, 117; e) V. Balzani, A. Credi, M. Venturi, *ChemSusChem* **2008**, *1*, 26; f) D. Gust, T. A. Moore, A. L. Moore, *Acc. Chem. Res.* **2001**, *34*, 40; g) J. L. Sessler, C. M. Lawrence, J. Jayawickramarajah, *Chem. Soc. Rev.* **2007**, *36*, 314; h) S. Fukuzumi, K. Ohkubo, *J. Mater. Chem.* **2012**, *22*, 4575; i) *Photochemical Conversion and Storage of Solar Energy* (Ed.: J. S. Connolly), Academic Press, New York, **1981**.

[3] a) D. M. Guldi, G. M. A. Rahman, F. Zerbetto, M. Prato, *Acc. Chem. Res.* **2005**, *38*, 871; b) L. Sánchez, N. Martín, D. M. Guldi, *Angew. Chem. Int. Ed.* **2005**, *44*, 5374; *Angew. Chem.* **2005**, *117*, 5508; c) S. Fukuzumi, *Phys. Chem. Chem. Phys.* **2008**, *10*, 2283; d) M. E. El-Khouly, O. Ito, P. M. Smith, F. D'Souza, *J. Photochem. Photobiol. C* **2004**, *5*, 79; e) M. R. Wasielewski, *Acc. Chem. Res.* **2009**, *42*, 1910; f) D. I. Schuster, K. Li, D. M. Guldi, *C. R. Chemie* **2006**, *9*, 892; g) S. Fukuzumi, K. Ohkubo, F. D'Souza, J. L. Sessler, *Chem. Commun.* **2012**, *48*, 9801.

[4] a) D. Gust, T. A. Moore, A. L. Moore, *Acc. Chem. Res.* **2009**, *42*, 1890; b) G. Bottari, G. de La Torre, D. M. Guldi, T. Torres, *Chem. Rev.* **2010**, *110*, 6768; c) D. M. Guldi, R. D. Costa, *J. Phys. Chem. Lett.* **2013**, *4*, 1489; d) A. Satake, Y. Kobuke, *Org. Biomol. Chem.* **2007**, *5*, 1679; e) H. Imahori, T. Umeyama, K. Kei, T. Yuta, *Chem. Commun.* **2012**, *48*, 4032; f) F. D'Souza, O. Ito, *Chem. Soc. Rev.* **2012**, *41*, 86; g) S. Fukuzumi, *Org. Biomol. Chem.* **2003**, *1*, 609; h) N. V. Tkachenko, H. Lemmetyinen in *Handbook of Carbon Nanomaterials* (Eds.: F. D'Souza, K. Kadish), World Scientific Publications, Singapore, **2011**, Chapter 13, pp. 405–440; i) G. de La Torre, P. Vazquez, F. Agullo-Lopez, T. Torres, *Chem. Rev.* **2004**, *104*, 3723.

[5] a) T. Umeyama, H. Imahori, *Energy Environ. Sci.* **2008**, *1*, 120; b) N. S. Lewis, D. G. Nocera, *Proc. Natl. Acad. Sci. USA* **2006**, *103*, 15729; c) P. V. Kamat, *J. Phys. Chem. C* **2007**, *111*, 2834; d) T. Hasobe, *Phys. Chem. Chem. Phys.* **2010**, *12*, 44; e) V. Balzani, A. Credi, M. Venturi in *Organic Nanostructures* (Eds.: J. L. Atwood, J. W. Steed), Wiley-VCH, Weinheim; **2008**, pp. 1–31; f) *Energy Harvesting Materials* (Ed.: D. L. Andrews), World Scientific, Singapore, **2005**; g) J. Barber, *Chem. Soc. Rev.* **2009**, *38*, 185.

[6] a) *Introduction of Molecular Electronics* (Eds.: M. C. Petty, M. R. Bryce, D. Bloor), Oxford University Press, New York, **1995**; b) A. Aviram, B. Davis, M. Kemp, V. Mujica, A. Roitberg, S. Yaliraki, *Ann. NY Acad. Sci.* **1998**, *852*, 22; c) *Molecular Switches* (Ed.: B. L. Feringa), Wiley-VCH, Weinheim, **2001**; d) D. Gust, T. A. Moore, A. L. Moore, *Chem. Commun.* **2006**, *11*, 1169; e) V. Balzani, A. Credi, M. Venturi, in *Organic Nanostructures* (Eds.: J. L. Atwood, J. W. Steed), Wiley-VCH, Weinheim, **2008**, pp. 1–31; f) J. M. Tour, *Molecular Electronics; Commercial Insights, Chemistry, Devices, Architectures and Programming*, World Scientific, River Edge, **2003**; g) J. S. Lindsey, D. F. Bocian, *Acc. Chem. Res.* **2011**, *44*, 638; h) F. D'Souza, O. Ito, *Chem. Commun.* **2009**, 4913.

[7] a) *The Photosynthetic Reaction Center* (Eds.: J. Deisenhofer, J. R. Norris), Academic Press, New York, **1993**; b) *Molecular Mechanism of Photosynthesis* (Ed.: R. E. Blankenship), Blackwell Science, Oxford, **2002**.

[8] a) H. Imahori, D. M. Guldi, K. Tamaki, Y. Yoshida, C. Luo, Y. Sakata, S. Fukuzumi, *J. Am. Chem. Soc.* **2001**, *123*, 6617; b) H. Imahori, K. Tamaki, D. M. Guldi, C. Luo, M. Fujitsuka, O. Ito, Y. Sakata, S. Fukuzumi, *J. Am. Chem. Soc.* **2001**, *123*, 2607; c) F. D'Souza, E. Maligaspe, K. Ohkubo, M. E. Zandler, N. K. Subbaiyan, S. Fukuzumi, *J. Am. Chem. Soc.* **2009**, *131*, 8787; d) M. E. El-Khouly, C. A. Wijesinghe, V. N. Nesterov, M. E. Zandler, S. Fukuzumi, F. D'Souza, *Chem. Eur. J.* **2012**, *18*, 13844; e) G. N. Lim, E. Maligaspe, M. E. Zandler, F. D'Souza, *Chem. Eur. J.* **2014**, *20*, 17089; f) C. B. KC, G. N. Lim, F. D'Souza, *Nanoscale* **2015**, *7*, 6813; g) C. B. KC, G. N. Lim, F. D'Souza, *Angew. Chem. Int. Ed.* **2015**, *54*, 5088; *Angew. Chem.* **2015**, *127*, 5177.

[9] a) A. Dualeh, J. H. Delcamp, M. K. Nazeeruddin, M. Grätzel, *Appl. Phys. Lett.* **2012**, *100*, 173512; b) E. Arunkumar, A. Ajayaghosh, *Chem. Commun.* **2005**, *5*, 599; c) V. Bandi, S. K. Das, S. G. Awuah, Y. You, F. D'Souza, *J. Am. Chem. Soc.* **2014**, *136*, 7571.

[10] a) A. Treibs, F. H. Kreuzer, *Justus Liebigs Ann. Chem.* **1968**, *718*, 208; b) A. Loudet, K. Burgess, *Chem. Rev.* **2007**, *107*, 4891; c) N. Boens, V. Leen, W. Dehaen, *Chem. Soc. Rev.* **2012**, *41*, 1130; d) M. Tasior, D. F. O'Shea, *Bioconjugate Chem.* **2010**, *21*, 1130; e) M. Grossi, A. Palma, S. O. McDonnell, M. J. Hall, D. K. Rai, J. Muldoon, D. F. O'Shea, *J. Org. Chem.* **2012**, *77*, 9304.

© 2015 Wiley-VCH Verlag GmbH & Co. KGaA, Weinheim

[11] a) G. Ulrich, R. Ziessel, A. Harriman, *Angew. Chem. Int. Ed.* **2008**, *47*, 1184; *Angew. Chem.* **2008**, *120*, 1202; b) R. Ziessel, A. Harriman, *Chem. Commun.* **2011**, *47*, 611; c) M. E. El-Khouly, S. Fukuzumi, F. D'Souza, *ChemPhysChem* **2014**, *15*, 30.

[12] a) F. Li, S. I. Yang, T. Ciringh, J. Seth, C. H. Martin III, D. L. Singh, D. Kim, R. R. Birge, D. F. Bocian, D. Holten, J. S. Lindsey, *J. Am. Chem. Soc.* **1998**, *120*, 10001; b) C. B. KC, G. N. Lim, V. N. Nesterov, P. A. Karr, F. D'Souza, *Chem. Eur. J.* **2014**, *20*, 17100 and references cited therein.

[13] a) S. O. McDonnell, M. J. Hall, L. T. Allen, A. Byrne, W. M. Gallagher, D. F. O'Shea, *J. Am. Chem. Soc.* **2005**, *127*, 16360; b) K. Flavin, K. Lawrence, J. Bartelmess, M. Tasior, C. Navio, C. Bittencourt, D. F. O'Shea, D. M. Guldi, S. Giordani, *ACS Nano* **2011**, *5*, 1198.

[14] a) W.-J. Shi, R. Menting, E. A. Ermilov, P. C. Lo, B. Roeder, D. K. P. Ng, *Chem. Commun.* **2013**, *49*, 5277; b) W.-J. Shi, M. E. El-Khouly, K. Ohkubo, S. Fukuzumi, D. K. P. Ng, *Chem. Eur. J.* **2013**, *19*, 11332; c) M. Yuan, X. Yin, H. Zheng, C. Ouyang, Z. Zuo, H. Liu, Y. Li, *Chem. Asian J.* **2009**, *4*, 707; d) P. A. Bouit, K. Kamada, P. Feneyrou, G. Berginc, L. Toupet, O. Maury, C. Andraud, *Adv. Mater.* **2009**, *21*, 1151; e) S. Y. Leblebici, L. Catane, D. E. Barclay, T. Olson, T. L. Chen, B. Ma, *ACS Appl. Mater. Interfaces* **2011**, *3*, 4469; f) K. Flavin, I. Kopfa, J. Murtagh, M. Grossi, D. F. O'Shea, S. Giordani, *Supramol. Chem.* **2012**, *24*, 23.

[15] a) A. N. Amin, M. E. El-Khouly, N. K. Subbaiyan, M. E. Zandler, M. Supur, S. Fukuzumi, F. D'Souza, *J. Phys. Chem. A* **2011**, *115*, 9810; b) M. E. El-Khouly, A. N. Amin, M. E. Zandler, S. Fukuzumi, F. D'Souza, *Chem. Eur. J.* **2012**, *18*, 5239; c) A. N. Amin, M. E. El-Khouly, N. K. Subbaiyan, M. E. Zandler, S. Fukuzumi, F. D'Souza, *Chem. Commun.* **2012**, *48*, 206; d) F. D'Souza, A. N. Amin, M. E. El-Khouly, N. K. Subbaiyan, M. E. Zandler, S. Fukuzumi, *J. Am. Chem. Soc.* **2012**, *134*, 654; e) V. Bandi, K. Ohkubo, S. Fukuzumi, F. D'Souza, *Chem. Commun.* **2013**, *49*, 2867; f) V. Bandi, M. E. El-Khouly, V. N. Nesterov, P. A. Karr, S. Fukuzumi, F. D'Souza, *J. Phys. Chem. C* **2013**, *117*, 5638; g) V. Bandi, M. E. El-Khouly, K. Ohkubo, V. N. Nesterov, M. E. Zandler, S. Fukuzumi, F. D'Souza, *Chem. Eur. J.* **2013**, *19*, 7221; h) V. Bandi, H. B. Gobeze, P. A. Karr, F. D'Souza, *J. Phys. Chem. C* **2014**, *118*, 18969; i) V. Bandi, H. B. Gobeze, V. N. Nesterov, P. A. Karr, F. D'Souza, *Phys. Chem. Chem. Phys.* **2014**, *16*, 25537; j) V. Bandi, F. P. D'Souza, H. B. Gobeze, F. D'Souza, *Chem. Eur. J.* **2014**, *20*, 1; k) V. Bandi, H. B. Gobeze, V. Lakshmi, M. Ravikanth, *J. Phys. Chem. C* **2015**, *119*, 8095.

[16] a) R. Gresser, M. Hummert, H. Hartmann, K. Leo, M. Riede, *Chem. Eur. J.* **2011**, *17*, 2939; b) H. Lu, S. Shimizu, J. Mack, Z. Shen, N. Kobayashi, *Chem. Asian J.* **2011**, *6*, 1026; c) X. Zhang, H. Yu, Y. Xiao, *J. Org. Chem.* **2012**, *77*, 669.

[17] a) H. W. Kroto, J. R. Heath, S. C. O'Brien, R. F. Curl, R. E. Smalley, *Nature* **1985**, *318*, 162; b) R. E. Smalley, *Angew. Chem. Int. Ed. Engl.* **1997**, *36*, 1594; *Angew. Chem.* **1997**, *109*, 1666; c) Q. Xie, E. Perez-Cordero, L. Echegoyen, *J. Am. Chem. Soc.* **1992**, *114*, 3978.

[18] M. Maggini, G. Scorrano, M. Prato, *J. Am. Chem. Soc.* **1993**, *115*, 9798.

[19] *Gaussian 03*, M. J. Frisch, G. W. Trucks, H. B. Schlegel, G. E. Scuseria, M. A. Robb, J. R. Cheeseman, V. G. Zakrzewski, J. A. Montgomery, R. E. Stratmann, J. C. Burant, S. Dapprich, J. M. Millam, A. D. Daniels, K. N. Kudin, M. C. Strain, O. Farkas, J. Tomasi, V. Barone, M. Cossi, R. Cammi, B. Mennucci, C. Pomelli, C. Adamo, S. Clifford, J. Ochterski, G. A. Petersson, P. Y. Ayala, Q. Cui, K. Morokuma, D. K. Malick, A. D. Rabuck, K. Raghavachari, J. B. Foresman, J. Cioslowski, J. V. Ortiz, B. B. Stefanov, G. Liu, A. Liashenko, P. Piskorz, I. Komaromi, R. Gomperts, R. L. Martin, D. J. Fox, T. Keith, M. A. Al-Laham, C. Y. Peng, A. Nanayakkara, C. Gonzalez, M. Challacombe, P. M. W. Gill, B. G. Johnson, W. Chen, M. W. Wong, J. L. Andres, M. Head-Gordon, E. S. Replogle, J. A. Pople, Gaussian, Inc., Pittsburgh PA, **2003**.

[20] For a general review on DFT applications of porphyrin-fullerene systems see: M. E. Zandler, F. D'Souza, *C. R. Chemie* **2006**, *9*, 960.

[21] a) D. Rehm, A. Weller, *Isr. J. Chem.* **1970**, *8*, 259; b) N. Mataga, H. Miyasaka, in *Electron Transfer* (Eds.: J. Jortner, M. Bixon), John Wiley & Sons, New York, **1999**, Part 2, pp. 431 – 496.

[22] Phosphorescence spectrum of ADP, BADP, and TADP in the presence of CH_3I did not show any peaks in the range of 700–1200 nm, which suggests that the energy triplet levels lie below 1.0 eV. For the phosphorescence spectrum of BDP, the value reported for halogenated BDP was employed, see Ref. [23].

[23] X.-F. Zhang, X. Yang, K. Niu, H. Geng, *J. Photochem. Photobiol. A* **2014**, *285*, 16.

[24] *Principles of Fluorescence Spectroscopy*, 3rd ed. (Ed.: J. R. Lakowicz), Springer, Singapore, **2006**.

[25] a) C. A. Wijesinghe, M. E. El-Khouly, J. D. Blakemore, M. E. Zandler, K. Fukuzumi, F. D'Souza, *Chem. Commun.* **2010**, *46*, 3301; b) C. A. Wijesinghe, M. E. El-Khouly, N. K. Subbaiyan, M. Supur, M. E. Zandler, K. Ohkubo, S. Fukuzumi, F. D'Souza, *Chem. Eur. J.* **2011**, *17*, 3147.

[26] F. D'Souza, R. Chitta, K. Ohkubo, M. Tasior, N. K. Subbaiyan, M. E. Zandler, M. K. Rogachi, D. T. Gryko, S. Fukuzumi, *J. Am. Chem. Soc.* **2008**, *130*, 14263.

[27] R. A. Marcus, N. Sutin, *Biochimica. Biophys. Acta* **1985**, *811*, 265.

Received: February 21, 2015
Published online on June 30, 2015

© 2015 Wiley-VCH Verlag GmbH & Co. KGaA, Weinheim